PHOTONICS Research

Multi-wavelength random fiber laser with a spectral-flexible characteristic

Sicheng Li,[1] Jiangming Xu,[1,2] Junrui Liang,[1] Jun Ye,[1] Yang Zhang,[1] Xiaoya Ma,[1] Jinyong Leng,[1] and Pu Zhou[1,3]

[1]College of Advanced Interdisciplinary Studies, National University of Defense Technology, Changsha 410073, China
[2]e-mail: jmxu1988@163.com
[3]e-mail: zhoupu203@163.com

Received 12 September 2022; revised 15 November 2022; accepted 22 November 2022; posted 23 November 2022 (Doc. ID 475233); published 23 January 2023

In past decades, multi-wavelength lasers have attracted much attention due to their wide applications in many fields. In this paper, we demonstrate a multi-wavelength random fiber laser with customizable spectra enabled by an acousto–optic tunable filter. The operating wavelength range can be tuned from 1114.5 to 1132.5 nm with a maximal output power of 5.55 W, and spectral channel tuning can also be realized with a maximal number of five. The effect of gain competition and the interaction between Raman gain and insertion loss are also analyzed. Furthermore, the output spectra can be ordered by radiating appropriate radio frequency signals to the acousto–optic tunable filter. This work may provide a reference for agile shape spectrum generation and promote multi-wavelength random fiber laser practicability in sensing, telecommunications, and precise spectroscopy.

https://doi.org/10.1364/PRJ.475233

1. INTRODUCTION

The random fiber laser (RFL), which was proposed by Turitsyn *et al.* in 2010 [1], has had fast growth in its development and practical applications [2–4]. In recent years, RFLs have advanced in many areas, including high-power output [5,6], wavelength tuning [7,8], *Q*-switching [9], linearly polarized operation [10,11], dynamics of intensity fluctuation transfer [12], and so on [2–4]. Among the various researches on RFLs, multi-wavelength operation is a hotspot due to its promising applications in optical communication, precise spectroscopy, optical sensing, and microwave generation [13–15]. RFLs also show great potential for generating multi-wavelength output [4,12,16–18]. The special power distribution property of RFL makes it possible to conduct spectral manipulation of high-power laser output with low-power-capability spectral tuning devices [19]. The broad and flat gain with a wave band insensitive feature also benefits tunable multi-wavelength generation at many customizable wavelengths [8,20–23]. In addition, compared with rare-earth-doped fiber lasers, whose working wave bands are partly limited by the emission spectra of the rare-earth dopants, RFL is a promising flexible laser source in the transparency window of the fiber [4,16].

Various kinds of RFL schemes have been demonstrated to realize wavelength tunability [19,20,24–28], including inserting a tunable filter into the cavity [20], employing an optical grating filter [26], and combining a fiber Fabry–Perot cavity with a Mach–Zehnder interferometer [27]. A tunable pump source is combined with the cascaded stimulated Raman scattering process to further widen the wavelength tuning range [25]. A cascaded random Raman fiber laser using a comb filter can also realize spectral manipulation [28]. Apart from the selection of wavelength, there are already a variety of structures for implementing multi-wavelength generation of fiber lasers. Common methods include the stimulated Brillouin scattering effect [29,30], four-wave mixing effect [31], Mach–Zehnder interferometer [32], Sagnac loop mirror [33], Fabry–Perot interferometer [34], fiber Bragg grating [35,36], two-dimensional materials [37], ultra-long-period grating [38], nonlinear amplifying loop mirror [39], and Loyt filter [22]. However, flexible wavelength tuning and multi-wavelength generation can hardly be obtained simultaneously.

Fortunately, the acousto-optic tunable filter (AOTF) can offer effective access to generate multi-wavelength lasing while achieving flexible wavelength choices and wavelength-dependent loss. The central wavelength and corresponding loss can be controlled by designing radio frequency (RF) signals [40]. Since its advent, AOTF has been widely applied in different fields [40–43]. Flexible multi-wavelength tuning has been actualized based on an ytterbium-doped fiber, whose tuning range reaches 1032–1111 nm [44,45]. In addition, a tunable multi-wavelength erbium-doped fiber laser has also been realized with a tuning range from 1524 to 1567 nm [46]. Overall,

few wavelength-tunable fiber lasers have been realized based on this multifunction device [47,48]. Furthermore, there is no report of an AOTF used for cavity-free RFL to achieve flexible multi-wavelength output. But it is anticipated that the flexible tuning capability makes AOTF a versatile device for spectral filtering and manipulation, which enables a multi-wavelength RFL employed by an AOTF to achieve high-power-spectrum editable random laser output.

In this paper, a spectrum-customizable multi-wavelength RFL enabled by an AOTF is demonstrated. The central wavelength can be tuned from 1114.5 to 1132.5 nm by adjusting the frequency of the RF signal loaded on the AOTF. In addition, the number of lasing wavelengths, which is controlled by the channel number of RF signals, can be adjusted from one to five. The linewidth can be widened to 4.5 nm, and each wavelength component can be tuned independently to achieve spectral-flexible output.

2. EXPERIMENTAL SETUP

The schematic of the spectral-flexible multi-wavelength RFL is shown in Fig. 1. A homemade high-power amplified spontaneous emission (ASE) source is adopted as the pump light, whose working bandwidth is 15.2 nm and centered at 1065 nm [49]. A roll of 3 km passive fiber is applied to provide Raman gain and random distributed feedback. The core and cladding diameters of the passive fiber are 9 and 125 μm, respectively. The numerical aperture (NA) of the fiber core is 0.14, and the attenuation coefficient is about 0.7 dB/km when the central wavelength is between 1050 and 1150 nm. A 1070/1120 nm wavelength division multiplexer (WDM) is inserted between the pump source and passive fiber to separate the backward scattering Stokes light component from the pump light. The 1070 nm port of WDM is connected with the ASE source while the 1120 nm port is connected with a feedback loop composed of a circulator and an AOTF. The backward Stokes light component is used as feedback light that enters the circulator from port 2 and is output at port 3, and then it is filtered by the AOTF. After filtering, the feedback light enters the circulator from port 1 and is output at port 2, and then is injected into the passive fiber through the WDM. An optical spectrum analyzer (OSA) and a power monitor (PM) are respectively adopted to measure the output spectrum and power after the output port.

Due to the adoption of a wide bandwidth pump source, the gain spectrum of the passive fiber is flat and has a characteristic of high-middle and low-edge gain [22]. In the operation, to obtain multi-wavelength outputs with equal amplitudes, we adjust the applied voltage to make the loss at the middle wavelengths higher and the loss at the edge wavelengths lower in the AOTF transmission spectrum. The spectra in Fig. 1 show the process of multi-wavelength output with equal amplitudes enabled by controlling the transmission spectrum of AOTF. The edges of the filtered spectrum have higher transmittance, which corresponds to the wave band of the gain spectrum having lower gain. Conversely, the filtering loss is higher in the region with higher gain. The interaction between the two results in multi-wavelength output with equal amplitude.

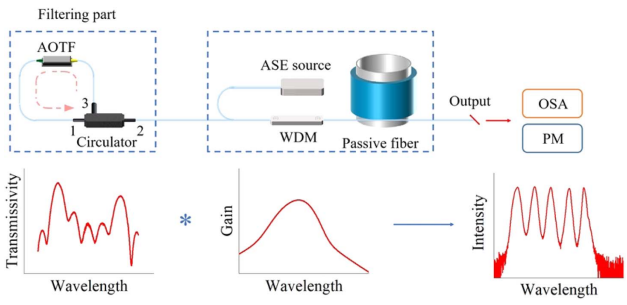

Fig. 1. Schematic diagram and operation principle of multi-wavelength RFL.

3. RESULTS AND DISCUSSION

A. Single-Wavelength Output and Central Wavelength Tuning

First, we measured the transmission spectrum of the AOTF. The first-order Raman laser that corresponds to the common 1070 nm pump source is about 1123 nm in this investigation, and we display the corresponding filtered spectrum of AOTF in Fig. 2(a). The full width at half maximum (FWHM) linewidth of the main peak is 2.0 nm, and several sidebands appear beside the main peak. The wavelength interval between the main peak and secondary peak is about 5 nm, and the amplitude difference is about 12 dB.

Then, we measured the power and spectral evolution characteristics when the pump wavelength is about 1070 nm and the signal light wavelength is 1123 nm. As shown in Figs. 2(b) and 2(c), it can be observed that when the pump power exceeds 3.87 W, the 1070 nm component of the output power decreases rapidly and transforms into a 1.1 μm random laser quickly. When the pump power reaches 8.45 W, the 1.1 μm random laser achieves a maximal power of 4.67 W, corresponding to a conversion efficiency of 55.3%. As the

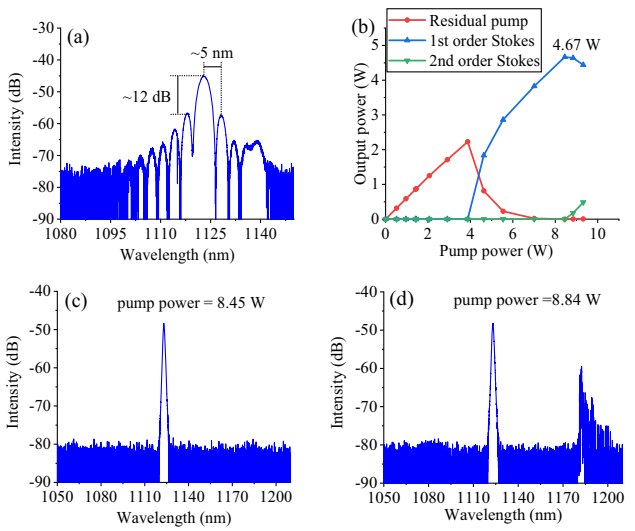

Fig. 2. (a) Filtered spectrum of AOTF at the central wavelength of 1123.0 nm. (b) Power evolution under different pump powers at the central wavelength of 1123 nm. Output spectrum of 1123 nm lasing at pump power levels of (c) 8.45 W and (d) 8.84 W.

passive fiber can introduce about 40% power loss with a transmission loss coefficient of about 0.7 dB/km and 3 km length, the conversion efficiency is mainly limited by the loss of the passive fiber. Figure 2(c) depicts the spectrum when the 1.1 μm random laser achieves its maximum (4.67 W). The central wavelength is 1123 nm and the FWHM is 1.08 nm. It is obvious that the sidebands of the feedback light are suppressed and the main peak is narrowed for the gain competition in the passive fiber [50]. The SNR is more than 30 dB, and the measured highest spectral purity is close to 100% in this case, where the ASE pump source contributes significantly. With further growth of pump power, the 1.1 μm random laser component will convert into the next order, and the output power of the first order Stokes component will be reduced, as presented in Fig. 2(d). Since the wavelength component of the next order is beyond the operating range of devices such as circulators, the pumping power was not further increased to avoid system damage. This means that the output power is limited by the generation of the next order Stokes component. By shortening the length of the passive fiber and increasing the core diameter, the stimulated Raman scattering threshold can be effectively increased, resulting in higher output power. However, it also greatly increases the power of the backward scattering light, which may exceed the power tolerance of AOTF. Hence, further optimization of the system structure is needed to achieve higher output power.

In this scheme, central wavelength tuning is easily achieved just by adjusting the frequency of the RF signal. As the frequency of the RF signal is continuously adjusted from 60.766 to 59.69 MHz, the central wavelength of the RFL varies from 1115 to 1132 nm, accordingly. Figure 3(a) displays the output spectra at different central wavelengths; the FWHM linewidth of each spectrum is between 1.08 and 1.32 nm. The maximal output power is also changed with the adjustment of the central wavelength. The power fluctuations are less than 18% over the entire tuning range. With the improvement of output power at the margin of the tuning range, a significant spontaneous Raman peak occurs. As revealed in Fig. 3(b), the component of spontaneous Raman lasing appears at the wavelength corresponding to the gain peak of pump light. The SNR reduces rapidly to 13 and 10 dB, respectively. Therefore, the wavelength tuning range is limited by the reduced SNR due to spontaneous Raman radiation.

B. Dual-Wavelength Output Characteristics and Linewidth Adjustment

On the basis of an 18 nm tuning range with the introduced RF signal, dual-wavelength output can easily be achieved by adding a second channel; the corresponding central wavelength is decided by the frequencies of the dual-channel RF signal. Figure 4(a) displays dual-wavelength output spectra with a wavelength interval of 10 nm centered at 1118 and 1128 nm, whose SNR is more than 25 dB, and the major frequencies are located at 60.585 and 59.98 MHz. When the major frequencies are tuned to 60.357 and 60.06 MHz, the SNR decreases to about 15 dB and the interval is adjusted to 4 nm. The spectrum is displayed in Fig. 4(b). The output power is about 4.73 W with a fluctuation ratio of 4.53% when operating wavelength is tuned. Actually, we can obtain dual-wavelength outputs in any combination within the tuning range by adjusting the RF signal frequencies of both channels. It should be noted that the SNR will be reduced as the wavelength interval is further decreased. However, the corresponding lasing tends to merge so as not to be distinguished when the signal frequency of different channels is similar.

In the investigation, we further reduced the RF signal frequency interval to control the linewidth. A dual-channel RF signal, whose frequencies are located at 60.39 and 60.22 MHz with radio amplitudes of 23 and 24, is loaded on the AOTF. The corresponding filter spectrum of AOTF is plotted in Fig. 5(a). In such a situation, the spectral components corresponding to the two frequencies overlap and merge into a broader spectrum with an FWHM linewidth of about 5.7 nm. The laser output spectrum at this parameter condition is shown in Fig. 5(b), with an FWHM linewidth of about 4 nm, which may be influenced by the narrowing of the spectrum due to gain competition. As the number of RF frequencies is further increased to five, we obtain the output spectrum, as shown in Fig. 5(c). The FWHM linewidth of the output random laser increases to 4.5 nm, which is broader with a smaller percentage increase compared to dual-channel output, which may be the result of gain competition.

C. Multi-Wavelength Output and Spectral Shape Control

Enabled by this multifunctional AOTF, multi-wavelength tuning is also achievable. As the channel number of the RF signals increases, multi-channel filtering can be realized. Figure 6(a) displays the tri-wavelength output with equal amplitudes and five-wavelength output with similar amplitudes, whose

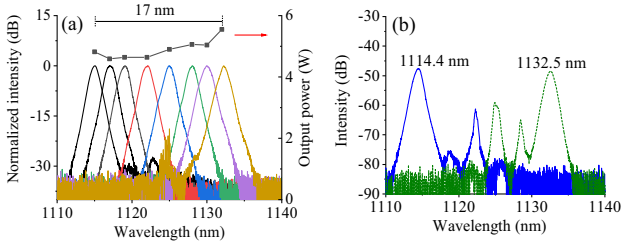

Fig. 3. (a) Output spectra at different central wavelengths and corresponding maximum output power. (b) Spontaneous Raman lasing appears while the central wavelengths are 1114.4 and 1132.5 nm.

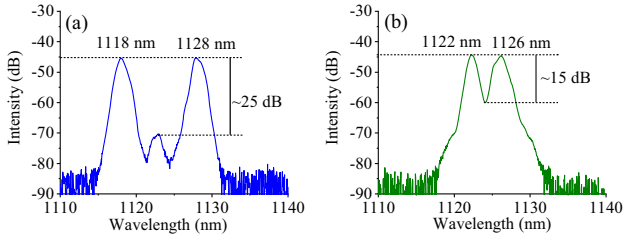

Fig. 4. Spectrum of dual-wavelength output with the interval of (a) 10 nm and (b) 4 nm.

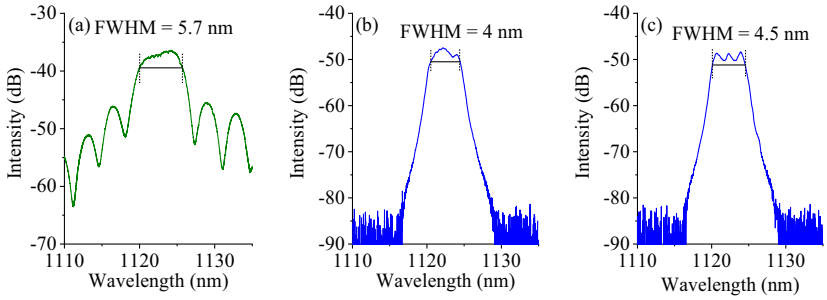

Fig. 5. (a) Filtered spectrum with dual-channel RF signal. Output spectra with FWHM of (b) 4 nm and (c) 4.5 nm.

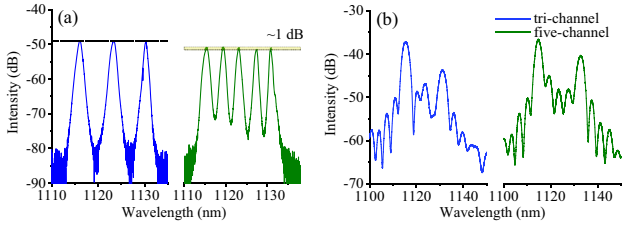

Fig. 6. (a) Spectra of tri-wavelength and five-wavelength output with equal/similar amplitude. (b) Corresponding filtered spectra.

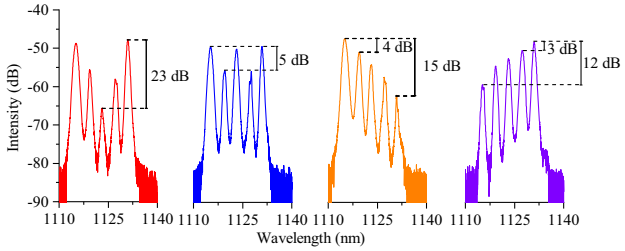

Fig. 7. Five-wavelength output with customized shape.

difference of relative wavelength is less than 1 dB. The tri-wavelength lasing spectrum is positioned at 1116, 1123, and 1130 nm, while the five-wavelength one is centered at 1115, 1119, 1123, 1127, and 1131 nm. The output powers are 5.17 and 5.03 W for tri-wavelength and five-wavelength output, respectively. Since the gain spectrum is not flat, we optimized the RF signal amplitude to obtain the transmission spectra, as shown in Fig. 6(b), in the experiments, to make up for the gain spectrum and get a laser line of equal amplitude.

In addition to the equal intensity multi-wavelength operation, variable intensity is also available from this multifunctional AOTF-based RFL. The output spectrum can be customized by adjusting the loading RF signals. Based on the five-wavelength equal-amplitude output, a spectrum with particular shapes, as plotted in Fig. 7, can be ordered by changing the radio amplitude. All spectra were measured at a pump power of 9.83 W, and the maximum power changes a little (~5 W) with the spectral profile. The output power is about 4.87 W with a fluctuation ratio of 3.29% when operating wavelength is tuned.

4. CONCLUSION

In conclusion, we have demonstrated an AOTF-enabled RFL with the characterization of wavelength selection and intensity tuning at the same time. The central wavelength can be operated in the range of 1114.5–1132.5 nm, and spectral channel tuning can also be realized with a maximal number of five. Even linewidth can be widened to 4.5 nm by the designed RF signal. Optimized loss of the filter makes up for the gain spectrum, leading to equal amplitude multi-wavelength outputs. Further adjustments allow us to obtain a customized spectral envelope. This spectrum-customizable multi-wavelength RFL has the potential of broadening the tuning wave band of tunable fiber lasers and promoting multi-wavelength RFLs' practicability in sensing, telecommunications, and precise spectroscopy.

Funding. Hunan Provincial Innovation Foundation for Postgraduate (CX20190006); Special Fund for Hunan Provincial Innovative Province Building (2019RS3017); National Natural Science Foundation of China (61905284).

Disclosures. The authors declare no conflicts of interest.

Data Availability. Data underlying the results presented in this paper are not publicly available at this time but may be obtained from the authors upon reasonable request.

REFERENCES

1. S. K. Turitsyn, S. A. Babin, A. E. El-Taher, P. Harper, D. V. Churkin, S. I. Kablukov, J. D. Ania-Castañón, V. Karalekas, and E. V. Podivilov, "Random distributed feedback fibre laser," Nat. Photonics **4**, 231–235 (2010).
2. S. K. Turitsyn, S. A. Babin, D. V. Churkin, I. D. Vatnik, M. Nikulin, and E. V. Podivilov, "Random distributed feedback fibre lasers," Phys. Rep. **542**, 133–193 (2014).
3. D. V. Churkin, S. Sugavanam, I. D. Vatnik, Z. Wang, E. V. Podivilov, S. A. Babin, Y. Rao, and S. K. Turitsyn, "Recent advances in fundamentals and applications of random fiber lasers," Adv. Opt. Photon. **7**, 516–569 (2015).
4. A. S. L. Gomes, A. L. Moura, C. B. de Araújo, and E. P. Raposo, "Recent advances and applications of random lasers and random fiber lasers," Prog. Quantum. Electron. **78**, 100343 (2021).
5. S. Du, T. Qi, D. Li, P. Yan, M. Gong, and Q. Xiao, "10 kW fiber amplifier seeded by random fiber laser with suppression of spectral broadening and SRS," IEEE Photon. Technol. Lett. **34**, 721–724 (2022).
6. H. Zhang, J. Wu, Y. Wan, P. Wang, B. Yang, X. Xi, X. Wang, and P. Zhou, "Kilowatt random Raman fiber laser with full-open cavity," Opt. Lett. **47**, 493–496 (2022).

7. H. Wu, W. Z. Wang, Y. Li, C. X. Li, J. Y. Yao, Z. N. Wang, and H. K. Liang, "Difference-frequency generation of random fiber lasers for broadly tunable mid-infrared continuous-wave random lasing generation," J. Lightwave Technol. **40**, 2965–2970 (2022).
8. Y. Zhang, J. Song, J. Ye, J. Xu, T. Yao, and P. Zhou, "Tunable random Raman fiber laser at 1.7 μm region with high spectral purity," Opt. Express **27**, 28800–28807 (2019).
9. S. Lin, Z. Wang, J. Li, S. Chen, Y. Rao, G. Peng, and A. S. L. Gomes, "Nonlinear dynamics of four-wave mixing, cascaded stimulated Raman scattering and self q-switching in a common-cavity ytterbium/Raman random fiber laser," Opt. Laser Technol. **134**, 106613 (2021).
10. E. A. Zlobina, S. I. Kablukov, and S. A. Babin, "Linearly polarized random fiber laser with ultimate efficiency," Opt. Lett. **40**, 4074–4077 (2015).
11. J. Xu, L. Huang, M. Jiang, J. Ye, P. Ma, J. Leng, J. Wu, H. Zhang, and P. Zhou, "Near-diffraction-limited linearly polarized narrow-linewidth random fiber laser with record kilowatt output," Photon. Res. **5**, 350–354 (2017).
12. J. Ye, X. Ma, Y. Zhang, J. Xu, H. Zhang, T. Yao, J. Leng, and P. Zhou, "Revealing the dynamics of intensity fluctuation transfer in a random Raman fiber laser," Photon. Res. **10**, 618–627 (2022).
13. T. Duan, H. Lan, H. Zhong, M. Zhou, R. Zhang, and F. Gao, "Hybrid multi-wavelength nonlinear photoacoustic sensing and imaging," Opt. Lett. **43**, 5611–5614 (2018).
14. Z. Wang, T. Wang, Q. Jia, W. Ma, Q. Su, and P. Zhang, "Triple Brillouin frequency spacing multiwavelength fiber laser with double Brillouin cavities and its application in microwave signal generation," Appl. Opt. **56**, 7419–7426 (2017).
15. H. Al-Taiy, N. Wenzel, S. Preußler, J. Klinger, and T. Schneider, "Ultra-narrow linewidth, stable and tunable laser source for optical communication systems and spectroscopy," Opt. Lett. **39**, 5826–5829 (2014).
16. H. Chen, S. Gao, M. Zhang, J. Zhang, L. Qiao, T. Wang, F. Gao, X. Hu, S. Li, and Y. Zhu, "Advances in random fiber lasers and their sensing application," Sensors **20**, 6122 (2020).
17. P. Huang, X. Shu, and Z. Zhang, "Multi-wavelength random fiber laser with switchable wavelength interval," Opt. Express **28**, 28686–28695 (2020).
18. S. Saleh, N. A. Cholan, A. H. Sulaiman, and M. A. Mahdi, "Stable multiwavelength erbium-doped random fiber laser," IEEE J. Sel. Top. Quantum Electron. **24**, 0902106 (2018).
19. J. Ye, J. Xu, J. Song, H. Wu, H. Zhang, J. Wu, and P. Zhou, "Flexible spectral manipulation property of a high power linearly polarized random fiber laser," Sci. Rep. **8**, 2173 (2018).
20. S. A. Babin, A. E. El-Taher, P. Harper, E. V. Podivilov, and S. K. Turitsyn, "Tunable random fiber laser," Phys. Rev. A **84**, 021805 (2011).
21. A. E. El-Taher, P. Harper, S. A. Babin, D. V. Churkin, E. V. Podivilov, J. D. Ania-Castanon, and S. K. Turitsyn, "Effect of Rayleigh-scattering distributed feedback on multiwavelength Raman fiber laser generation," Opt. Lett. **36**, 130–132 (2011).
22. J. Ye, Y. Zhang, J. Xu, J. Song, T. Yao, H. Xiao, J. Leng, and P. Zhou, "Broadband pumping enabled flat-amplitude multi-wavelength random fiber laser," Opt. Lett. **45**, 1786–1789 (2020).
23. X. Ma, J. Xu, J. Ye, Y. Zhang, L. Huang, T. Yao, J. Leng, Z. Pan, and P. Zhou, "Cladding-pumped Raman fiber laser with 0.78% quantum defect enabled by phosphorus-doped fiber," High Power Laser Sci. Eng. **10**, e8 (2022).
24. L. Zhang, H. Jiang, X. Yang, W. Pan, and Y. Feng, "Ultra-wide wavelength tuning of a cascaded Raman random fiber laser," Opt. Lett. **41**, 215–218 (2016).
25. L. Zhang, H. Jiang, X. Yang, W. Pan, S. Cui, and Y. Feng, "Nearly-octave wavelength tuning of a continuous wave fiber laser," Sci. Rep. **7**, 42611 (2017).
26. A. R. Sarmani, R. Zamiri, M. H. Abu Bakar, B. Z. Azmi, A. W. Zaidan, and M. A. Mahdi, "Tunable Raman fiber laser induced by Rayleigh backscattering in an ultra-long cavity," J. Eur. Opt. Soc.-Rapid. **6**, 11043 (2011).
27. Y. Y. Zhu, W. L. Zhang, and Y. Jiang, "Tunable multi-wavelength fiber laser based on random Rayleigh back-scattering," IEEE Photon. Technol. Lett. **25**, 1559–1561 (2013).
28. H. Wu, B. Han, and Y. Liu, "Tunable narrowband cascaded random Raman fiber laser," Opt. Express **29**, 21539–21550 (2021).
29. L. Zhang, Y. Xu, P. Lu, S. Mihailov, L. Chen, and X. Bao, "Multi-wavelength Brillouin random fiber laser via distributed feedback from a random fiber grating," J. Lightwave Technol. **36**, 2122–2128 (2018).
30. J. Wang, J. Zhang, A. Wang, X. Jiang, J. Yao, and Q. Zhan, "Cascaded stimulated Brillouin scattering erbium-doped fiber laser generating orbital angular momentum beams at tunable wavelengths," Opt. Express **29**, 18408–18419 (2021).
31. T. Huang, X. Li, P. P. Shum, Q. J. Wang, X. Shao, L. Wang, H. Li, Z. Wu, and X. Dong, "All-fiber multiwavelength thulium-doped laser assisted by four-wave mixing in highly germania-doped fiber," Opt. Express **23**, 340–348 (2015).
32. Y. Guo, F. Yan, T. Feng, Q. Qin, D. Cheng, B. Guan, T. Li, C. Yu, H. Zhou, K. Kumamoto, and Y. Suo, "Multi-wavelength thulium-doped fiber laser at 2.05 μm incorporating a superimposed polarization-maintaining fiber Bragg grating," Infrared Phys Technol. **122**, 104046 (2022).
33. Y. Zhang, J. Ye, X. Ma, J. Xu, J. Song, T. Yao, and P. Zhou, "High power tunable multiwavelength random fiber laser at 1.3 μm waveband," Opt. Express **29**, 5516–5524 (2021).
34. A. M. Salman, S. K. Al-Hayali, R. A. Faris, and A. Al-Janabi, "Hybrid nanocomposite film provides FWM and Fabry Perot filter: towards multi-wavelength fiber laser generation in 1 μm region," Optik **242**, 167375 (2021).
35. L. Zhang, F. Yan, T. Feng, W. Han, B. Guan, Q. Qin, Y. Guo, W. Wang, Z. Bai, H. Zhou, and Y. Suo, "Six-wavelength-switchable narrow-linewidth thulium-doped fiber laser with polarization-maintaining sampled fiber Bragg grating," Opt. Laser Technol. **136**, 106788 (2021).
36. J. Ye, X. Ma, Y. Zhang, J. Xu, H. Zhang, T. Yao, J. Leng, and P. Zhou, "From spectral broadening to recompression: dynamics of incoherent optical waves propagating in the fiber," PhotoniX **2**, 15 (2021).
37. J. Liu, Y. Chen, Y. Li, H. Zhang, S. Zheng, and S. Xu, "Switchable dual-wavelength q-switched fiber laser using multilayer black phosphorus as a saturable absorber," Photon. Res. **6**, 198–203 (2018).
38. B. Guo, X. Guo, L. Tang, W. Yang, Q. Chen, and Z. Ren, "Ultra-long-period grating-based multi-wavelength ultrafast fiber laser [invited]," Chin. Opt. Lett. **19**, 071405 (2021).
39. Z. Guo, T. Liu, J. Peng, Y. Zhu, K. Huang, and H. Zeng, "Self-started dual-wavelength mode-locking with well-controlled repetition rate difference," J. Lightwave Technol. **39**, 3575–3581 (2021).
40. P. C. Shardlow, J. Ward, C. Pannell, S. Valle, and W. A. Clarkson, "Null-frequency-shift acousto-optic tunable filter for wavelength tuning of a tm fibre laser," in *European Conference on Lasers and Electro-Optics–European Quantum Electronics Conference* (2015), paper CJ_14_16.
41. M. Pawliszewska, M. R. Majewski, and S. D. Jackson, "Electronically tunable picosecond pulse generation from Ho^{3+}-doped fluoride fiber laser using frequency-shifted feedback," Opt. Lett. **45**, 5808–5811 (2020).
42. K. V. Zaichenko and B. S. Gurevich, "Spectral selection using acousto-optic tunable filters for the skin lesions diagnostics," in *European Conferences on Biomedical Optics (ECBO)* (2021), paper EM1A.8.
43. A. Machikhin, "Acousto-optical tunable filters: applications in 3D imaging and multi-wavelength digital holography," in *OSA Imaging and Applied Optics Congress (3D, COSI, DH, ISA, pcAOP)* (2021), paper DM5E.1.
44. W. Yue, T. Chen, W. Kong, Z. Ji, L. Yin, G. Huang, Z. He, and R. Shu, "Flexible wavelength generation from a Yb-doped fiber laser incorporating multifunctional acousto-optic tunable filter," Opt. Lett. **46**, 1041–1044 (2021).
45. S. Li, J. Xu, J. Liang, J. Ye, Y. Zhang, X. Ma, and P. Zhou, "High-power multi-wavelength Yb-doped fiber laser with a tunable interval, amplitude, and a number of channels," Opt. Lett. **47**, 4123–4126 (2022).
46. N. Hashimoto, H. Miyata, Y. Takasu, G. Han, T. Uematsu, and T. Nakazawa, "Tunable erbium-doped fiber ring laser using acousto-optic tunable filter," in *Integrated Photonics Research* (2001), paper ITuG4.

47. W. Yang, Y. Liu, L. Xiao, and Z. Yang, "Wavelength-tunable erbium-doped fiber ring laser employing an acousto-optic filter," J. Lightwave Technol. **28**, 118–122 (2010).
48. L. Huang, X. Song, P. Chang, W. Peng, W. Zhang, F. Gao, F. Bo, G. Zhang, and J. Xu, "All-fiber tunable laser based on an acousto-optic tunable filter and a tapered fiber," Opt. Express **24**, 7449–7455 (2016).
49. J. Ye, J. Xu, Y. Zhang, J. Song, J. Leng, and P. Zhou, "Spectrum-manipulable hundred-watt-level high-power superfluorescent fiber source," J. Lightwave Technol. **37**, 3113–3118 (2019).
50. J. Ye, Y. Zhang, J. Xu, J. Song, T. Yao, H. Xiao, J. Leng, and P. Zhou, "Investigations on the extreme frequency shift of phosphosilicate random fiber laser," J. Lightwave Technol. **38**, 3737–3744 (2020).